

PROGRESS REVIEW

High frequency dielectric materials for medicine and telecommunications

To cite this article: Michael T. Lanagan et al 2021 Jpn. J. Appl. Phys. 60 SF0801

View the article online for updates and enhancements.

You may also like

- Optoelectronic oscillator for 5G wireless networks and beyond
 Fang Zou, Lei Zou, Bo Yang et al.
- A Different Shaped Radiating Element Wide Band Multi-Band Massive MIMO Antenna for 5G/WLAN applications with Enhanced Correlation Coefficient Shrenik Suresh Sarade and S. D. Ruikar
- Research on millimeter wave spectrum planning for 5G
 Guoqin Kang, Shuiqiao Jiang and Zhiyuan Zhao

Check for updates

High frequency dielectric materials for medicine and telecommunications

Michael T. Lanagan¹, Tucker Brown¹, Steve Perini¹, and Qing X. Yang²

¹Materials Research Institute, Penn State University, University Park PA, United States of America

Received September 8, 2021; revised September 10, 2021; accepted September 15, 2021; published online October 1, 2021

The MHz–THz frequency range encompasses several important applications including magnetic resonance imaging (MRI) and wireless communications ferroelectric and paraelectric materials with high permittivity values have been applied to increase the sensitivity of MRI operating between 50 and 500 MHz. Low relative permittivity materials ($\varepsilon_r < 5$) with low dielectric loss are becoming more important for 5G applications above 6 GHz with an emphasis on low dielectric loss. © 2021 The Japan Society of Applied Physics

1. Introduction

The need for rapid image acquisition and data transmission has led to increased interest in developing new dielectric materials spanning MHz to THz frequencies. Magnetic resonance imaging (MRI) scan times for many clinical procedures can take up to one hour with patients remaining motionless. High permittivity dielectric materials placed between the coil and subject significantly increase the signal strength and potentially reduce the scan time. Paraelectric barium strontium titanate with high permittivity ($\varepsilon_r > 1000$) is a leading candidate for MRI dielectric pads that are placed on the body. Dielectric loss values in the 0.5%-2% range are acceptable for dielectric pads used this application because of the associated high loss biological tissue. For 5G and 6G applications above 6 GHz, temperature stable and low loss dielectric materials will be a priority. Miniaturization using high permittivity dielectrics is less of a concern for mm-wave devices. Polymer, glass and ceramic materials with loss values below 0.1% and permittivity values below 5 will be important for antennas, transmission lines and filters for frequencies approaching the THz range.

2. Broadband dielectric property characterization

Accurate permittivity and loss values are vital for the device simulation and design of 5G and MRI devices. ^{1,2)} Impedance spectroscopy at low frequency employs a parallel plate capacitor configuration and assumes a uniform electric field in the sample. Dielectric measurement methods at high frequency account for distributed electromagnetic fields because the sample dimensions are comparable to the electromagnetic wavelength. The dielectric measurement technique depends on sample geometry, frequency and loss magnitude and representative ranges are shown in Table I.

As frequencies increase above 300 MHz, the lumped characterization method is not applicable, and the distributed electric field must be considered. Resonant methods are generally discrete frequency measurements, have high accuracy, and are useful for low loss dielectrics. Transmission/reflection methods are carried out in coax, waveguide and free space configurations. Transmission/reflection methods have the advantage of being broadband extending over a large frequency range (10–100 GHz) and are pertinent to high loss materials. The resonant post method has been used extensively for ceramics since it is convenient for pressed and sintered shapes. Split-post and split-cavity techniques are compatible with substrates of arbitrary area that exceed a specified diameter. The open resonator is one of the most

useful techniques for 5G communication because is spans the mm-wave region and can characterize low loss dielectrics in the 10^{-5} range.

3. High permittivity ceramics for MRI in the MHz frequency range

The MRI research community has been investigating ways to enhance signal-to-noise-ratio (SNR) and decrease the scan time by integrating dielectric materials into coil arrays. High permittivity materials are currently being explored to increase the RF signal strength into the body by phase matching and enhancing the displacement current. We have investigated a range of $(Ba_xSr_{1-x})TiO_3 \ 0.4 < x < 0.6$ ceramics that were pressed into large diameter discs (8 cm diameter by 2 cm thick). The resonant post method was used to quantify a room-temperature permittivity value of 5000 with loss of 0.005 at 100 MHz for x = 0.6. This composition is applicable to conventional 1.5 T MRI using proton NMR signal at 64 MHz. The optimum permittivity is inversely related to the square of the MRI scanner frequency.

Ceramics and composites conformal to human anatomical shapes have been developed and utilized for increasing the SNR of cartilage MRI as shown in Fig. 1. A significant SNR increase was found in vivo in the patella and meniscal cartilage regions near the top of the knee where a conformal high-permittivity dielectric pad was placed, which greatly enhanced diagnostic sensitivity of cartilage degeneration. The SNR is critical for cartilage imaging where higher resolution is need because of it relatively smaller dimensions (2–4 mm in thickness). This technology can be also applied to general MRI in the brain and breast MRI. ¹⁸⁾

4. Dielectric materials for wireless communications mm-wave frequency range

The rapidly expanding 5G infrastructure will increase the need for antennas and transmission lines at frequencies greater than 28 GHz. Polymer, glass and ceramic substrates with relative permittivity values between $2<\varepsilon_{\rm r}<10$ and low dielectric loss are candidate substrates for patch antenna and coplanar transmission lines. $^{19,20)}$ In addition, propagation losses in building materials such as window glass is important to understand for the deployment of antenna arrays. $^{21)}$

Broadband dielectric properties are shown in Fig. 2 for quartz crystal, fused silica, window glass. Amorphous dielectrics such as fused silica and window glass have significantly higher loss than crystalline quartz which

²College of Medicine, Penn State University Hershey PA, United States of America

Technique	Frequency	Loss threshold	Sample geometry	References
Lumped element	Up to 300 MHz	10^{-2}	Substrate with electrode	3, 4
Distributed element	300 MHz-2 GHz	10^{-2}	Substrate with electrode	5
Resonant post	1-10 GHz	10^{-3}	Cylinder	6, 7
Split post	1-10 GHz	10^{-4}	Substrate	8
Split cavity	10-30 GHz	10^{-4}	Substrate	9, 10
Open resonator	20-100 GHz	10^{-5}	Substrate	11
Transmission/Reflection	10-100 GHz	10^{-2} to 10^{-3}	Waveguide and substrate	12–14

Table I. Dielectric measurement methods spanning the MHz to THz frequency range.



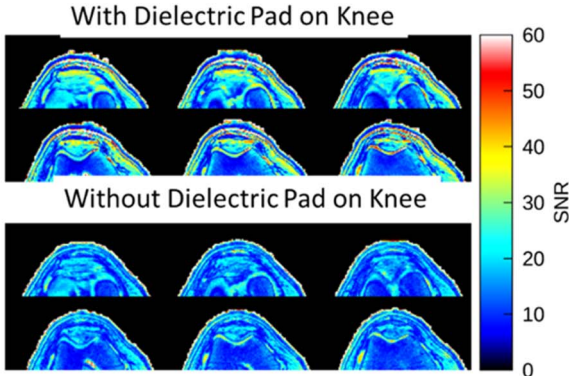


Fig. 1. (Color online) Left: A dielectric pad with $\varepsilon_r = 3500$ (blue color) was placed on the top of left knee of a young normal participant within a standard RF receive coil (left, anterior coil is not shown). Right: MRI SNR maps with (top) and without (bottom) dielectric pad. The SNR maps are normalized to the same color scale.

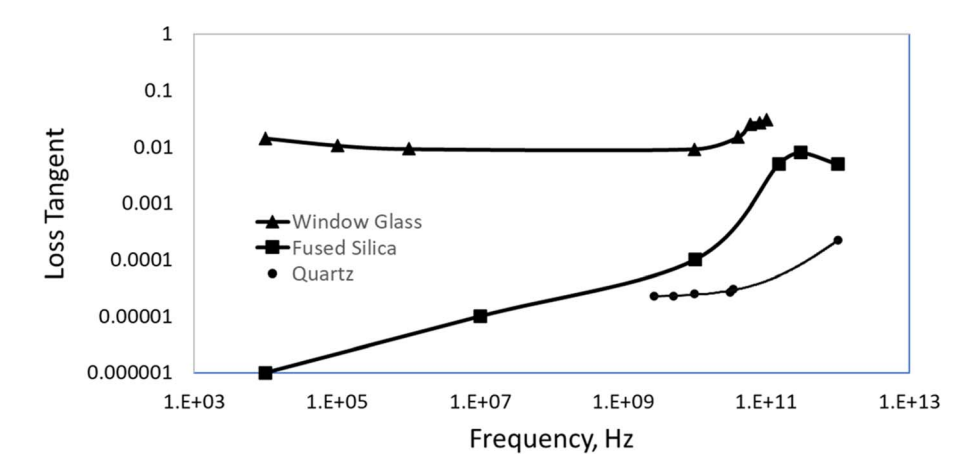


Fig. 2. (Color online) Broadband loss for glass and quartz. Capacitor, split cavity, and open resonator techniques spanned the frequency range between 10 and 100 GHz. Literature values were added to expand the low frequency range²²⁾ and the mm-wave region ^{11,23)} for fused silica.

remains low (tan $\delta = 2 \times 10^{-5}$) up to 50 GHz. Fused silica glass has low loss in the GHz frequency range (tan $\delta = 10^{-4}$) and the loss increases with frequency to 1% in the THz range. Window glass has high loss throughout the entire frequency range shown in Fig. 2, which has been attributed to alkali and alkaline earth modifiers in the silicate network former.

Dielectric relaxation mechanisms of amorphous and crystalline materials are fundamentally different. For high-purity crystalline dielectrics, the intrinsic loss in the microwave and mm-wave regimes is governed by the strength of frequency of IR lattice modes²⁴⁾ and anharmonic coupling and scattering of phonons.²⁵⁾ Amorphous silica has an additional polarization contribution from the Si–O unit that contributes to high loss in the GHz–THz frequency range.²⁶⁾ For window glass, sodium and calcium modifiers contribute to the additional loss, which can be associated with the additional ionic polarization in amorphous structures.²⁶⁾

5. Summary

New applications for dielectric materials will rely on a broad range of permittivity values. Ceramics with very large permittivity values ($\varepsilon_{\rm r} > 1000$) have been incorporated into MRI coil assemblies operating in the 10 to 100 MHz range. Low permittivity ($\varepsilon_{\rm r} < 10$) is of interest for telecommunication applications up to 100 GHz. It is interesting to note that the optimum permittivity values for these applications decrease by a factor of 10^2 whereas the frequency increases by 10^4 . This is fundamentally related to the electromagnetic wavelength being inversely related to the square root of the permittivity.

Acknowledgments

Financial support from the National Science Foundation as part of the Center for Dielectrics and Piezoelectrics under Grant Nos. IIP-1841453 and IIP-1841466. The magnetic

resonance imaging work was supported by the National Institutes of Health (NIH UO1 EB026978-01). The authors thank Sebastian Rupprecht HyQ Research Solutions, LLC for use of the dielectric pad.

Competing Interests

Q. X. Y. and M. T. L. are affiliated with HyQ Research Solutions, LLC, a manufacturer of dielectric ceramics and composites.

ORCID iDs

Michael T. Lanagan https://orcid.org/0000-0002-3274-1116

- D. Imran, M. M. Farooqi, M. I. Khattak, Z. Ullah, M. I. Khan, M. A. Khattak, and H. Dar, Presented at ICEET, Int. Conf. of Engineering and Emerging Technologies, 2018.
- K. Lakshmanan, G. Carluccio, J. Walczyk, R. Brown, S. Rupprecht, Q. X. Yang, M. T. Lanagan, and C. M. Collins, Magn. Reson. Med. 86, 1167 (2021).
- S. S. Stuchly, M. A. Rzepecka, and M. F. Iskander, IEEE Trans. Instrum. Meas. 23, 56 (1974).
- M. T. Lanagan, J. H. Kim, S. Jang, and R. E. Newnham, J. Am. Ceram. Soc. 71, 311 (1988).
- Š. Svirskas, D. Jablonskas, S. Rudys, S. Lapinskas, R. Grigalaitis, and J. Banys, Rev. Sci. Instrum. 91, 035106 (2020).
- B. W. Hakki and P. D. Coleman, IRE Trans. Microwave Theory Tech. 8, 402 (1960).
- 7) W. E. Courtney, IEEE Trans. Microwave Theory Tech. 18, 476 (1970).
- 8) J. Krupka, A. P. Gregory, O. C. Rochard, R. N. Clarke, B. Riddle, and J. Baker-Jarvis, J. Eur. Ceram. Soc. 21, 2673 (2001).

- 9) G. Kent, IEEE Trans. Microwave Theory Tech. 36, 1451 (1988).
- M. D. Janezic and J. Baker-Jarvis, IEEE Trans. Microwave Theory Tech. 47, 2014 (1999).
- 11) M. N. Asfar, IEEE Trans. Microwave Theory Tech. 32, 1598 (1984).
- M. T. Lanagan, N. Yang, D. C. Dube, and S. Jang, J. Am. Ceram. Soc. 72, 481 (1989).
- 13) Z. Lu, M. T. Lanagan, E. Manias, and D. D. Macdonald, J. Phys. Chem. B 113, 13551 (2009).
- 14) M. S. Hilario, B. W. Hoff, B. Jawdat, M. T. Lanagan, Z. W. Cohick, F. W. Dynys, J. A. Mackey, and J. M. Gaone, IEEE Trans. Compon., Packaging Manuf. Technol. 9, 1011 (2019).
- Q. X. Yang, J. Wang, J. Wang, C. M. Collins, C. Wang, and M. B. Smith, Magn. Reson. Med. 65, 358 (2011).
- S. Rupprecht, C. T. Sica, W. Chen, M. T. Lanagan, and Q. X. Yang, Magn. Reson. Med. 79, 2842 (2018).
- 17) W. Chen, B.-Y. Lee, X.-H. Zhu, H. M. Wiesner, M. Sarkarat, N. P. Gandji, S. Rupprecht, Q. X. Yang, and M. T. Lanagan, IEEE Trans. Med. Imaging 39, 3187 (2020).
- 18) A. Shchelokova et al., Nat. Commun. 11, 3840 (2020).
- M. S. Arunima, S. B. Nair, and K. U. Menon, Presented at ICCES, 5th Int. Conf. on Communication and Electronic Systems, 2020.
- M. T. Sebastian, Dielectric Materials for Wireless Communication (Elsevier, Amsterdam, 2010).
- 21) H. Kim and S. Nam, IEEE Antennas Wirel. Propag. Lett. 20, 108 (2020).
- 22) W. B. Westphal and A. Sils, Dielectric Constant and Loss Data Technical report (Air Force Materials Laboratory (U.S.)), AFML-TR-72-39 Wright-Patterson Air Force Base, Ohio: Air Force Materials Laboratory, Air Force Systems Command, 1972.
- D. Grischkowsky, S. Keiding, M. V. Exter, and C. Fattinger, JOSA B 7, 2006 (1990).
- 24) K. Wakino, M. Murata, and H. Tamura, J. Am. Ceram. Soc. 69, 34 (1986).
- A. K. Tagantsev, V. O. Sherman, K. F. Astafiev, J. Venkatesh, and N. Setter, J. Electroceram. 11. 5 (2003).
- M. T. Lanagan, L. Cai, L. A. Lamberson, J. Wu, E. Streltsova, and N. J. Smith, Appl. Phys. Lett. 116, 222902 (2020).